Enigmatic Nature of $\mathscr{B}$lack Holes

Relativistic Physics Seminar, BIMSA

Nishkal Rao

Indian Institute of Science Education and Research, Pune

nishkalrao20.github.io

March 9, 2026

Overview

Isolated Black Hole Horizons

Black Holes

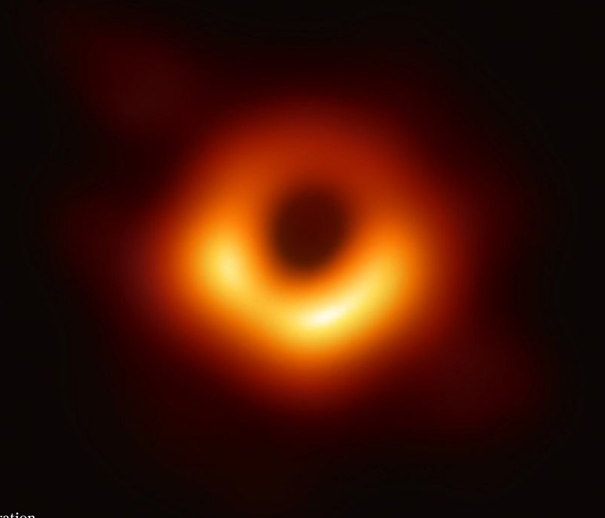

Event Horizon Telescope Collaboration

Defining the *Horizon*

Global Picture

Black Hole

For an *asymptotically flat* manifold $(\mathscr{M}, \boldsymbol{g})$, $\mathcal{B} = \mathscr{M} - J^{-}(\mathscr{I}^{+})$, the region of spacetime where light rays cannot escape to infinity.

Event Horizon

Boundary, $\partial J^{-}(\mathscr{I}^{+})$, smooth null hypersurface.

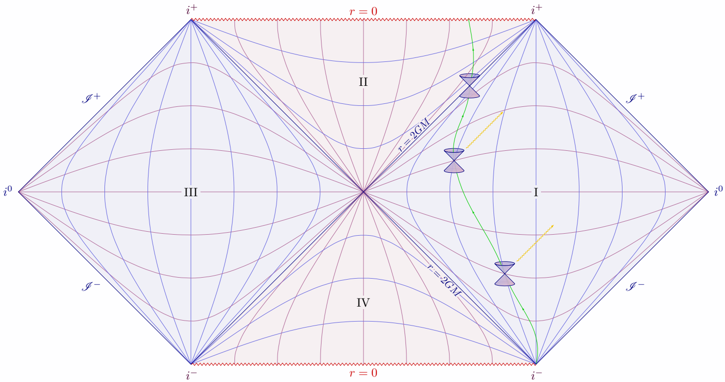

Null Geodesic Congruence

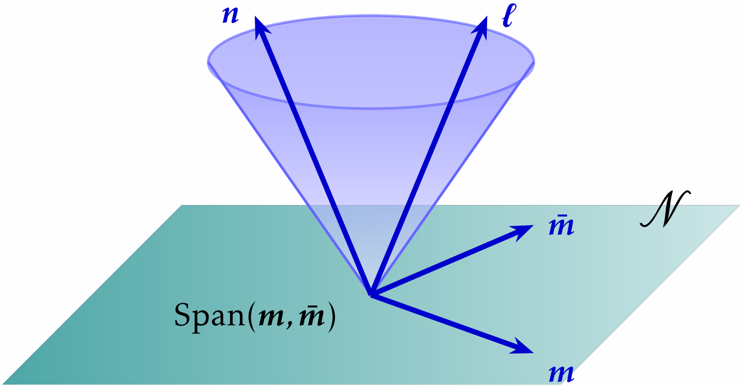

Newman-Penrose Tetrad

Orthonormal, Null tetrad $\{\boldsymbol{\ell}, \boldsymbol{n}, \boldsymbol{m}, \bar{\boldsymbol{m}}\}$.
Spacetime metric

$$\boldsymbol{g} = -\boldsymbol{\ell} \otimes \boldsymbol{n} - \boldsymbol{n} \otimes \boldsymbol{\ell} + \boldsymbol{m} \otimes \bar{\boldsymbol{m}} + \bar{\boldsymbol{m}} \otimes \boldsymbol{m}. \tag{1.1}$$

Induced metric $\boldsymbol{h} = \boldsymbol{g} + \underline{\boldsymbol{\ell}} \otimes \underline{\boldsymbol{n}} + \underline{\boldsymbol{n}} \otimes \underline{\boldsymbol{\ell}}$.

Encoding the Derivatives

$$
\begin{aligned}
d\boldsymbol{\ell} &= (\epsilon + \bar{\epsilon})\boldsymbol{\ell} \wedge \boldsymbol{n} + [\bar{\tau} - (\alpha + \bar{\beta})]\boldsymbol{\ell} \wedge \boldsymbol{m} + [\tau - (\bar{\alpha} + \beta)]\boldsymbol{\ell} \wedge \bar{\boldsymbol{m}} \\
&\quad + \bar{\kappa}\boldsymbol{n} \wedge \boldsymbol{m} + \kappa\boldsymbol{n} \wedge \bar{\boldsymbol{m}} + (\bar{\varrho} - \varrho)\boldsymbol{m} \wedge \bar{\boldsymbol{m}}, && \text{(1.2a)} \\
d\boldsymbol{n} &= (\gamma + \bar{\gamma})\boldsymbol{\ell} \wedge \boldsymbol{n} - \nu\boldsymbol{\ell} \wedge \boldsymbol{m} - \bar{\nu}\boldsymbol{\ell} \wedge \bar{\boldsymbol{m}} - [\pi - (\alpha + \bar{\beta})]\boldsymbol{n} \wedge \boldsymbol{m} \\
&\quad - [\bar{\pi} - (\bar{\alpha} + \beta)]\boldsymbol{n} \wedge \bar{\boldsymbol{m}} + (\bar{\mu} - \mu)\boldsymbol{m} \wedge \bar{\boldsymbol{m}}, && \text{(1.2b)} \\
d\boldsymbol{m} &= (\tau + \bar{\pi})\boldsymbol{\ell} \wedge \boldsymbol{n} - [\bar{\mu} + (\gamma - \bar{\gamma})]\boldsymbol{\ell} \wedge \boldsymbol{m} + \bar{\lambda}\boldsymbol{\ell} \wedge \bar{\boldsymbol{m}} \\
&\quad + [\varrho - (\epsilon - \bar{\epsilon})]\boldsymbol{n} \wedge \boldsymbol{m} + \sigma\boldsymbol{n} \wedge \bar{\boldsymbol{m}} + (\bar{\alpha} - \beta)\boldsymbol{m} \wedge \bar{\boldsymbol{m}}. && \text{(1.2c)}
\end{aligned}
$$

Focusing Light

$\mathbf{\Theta} = \nabla \underline{\boldsymbol{\ell}}$, Decomposition:

$$\mathbf{\Theta} = \frac{1}{2}\theta \boldsymbol{h} + \boldsymbol{\sigma} + \tilde{\boldsymbol{\omega}}, \tag{1.3}$$

1. $\theta = \mathrm{Tr}\vec{\mathbf{\Theta}} = h^{\mu\nu}\nabla_{\mu}\ell_{\nu}$ $\qquad \theta_{(\boldsymbol{\ell})} = 2\Re\varrho,\ \theta_{(\boldsymbol{n})} = -2\Re\mu$
2. $\sigma_{\alpha\beta} = \Theta_{(\alpha\beta)} - \frac{1}{2}\theta_{(\boldsymbol{\ell})}h_{\alpha\beta}$ $\qquad \sigma_{(\boldsymbol{\ell})} = \sigma,\ \sigma_{(\boldsymbol{n})} = -\lambda$
3. $\tilde{\omega}_{\alpha\beta} = \Theta_{[\alpha\beta]}$ $\qquad \tilde{\omega}_{(\boldsymbol{\ell})} = \Im\varrho,\ \tilde{\omega}_{(\boldsymbol{n})} = -\Im\mu$

Physical Picture

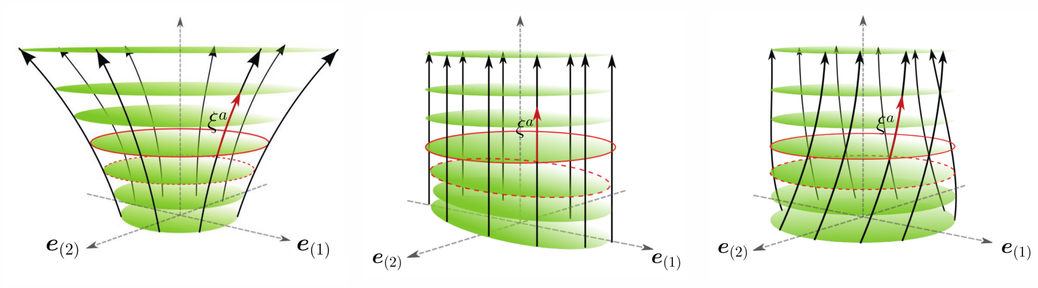

θ $\qquad$ $\boldsymbol{\sigma}$ $\qquad$ $\tilde{\omega}$

A. Ribes Metidieri. PhD thesis, Nijmegen U., 2025.

Dynamics of Light

Raychaudhuri equation:

$$\nabla_{\boldsymbol{\ell}}\theta_{(\boldsymbol{\ell})} = -\frac{1}{2}\theta_{(\boldsymbol{\ell})}^2 - \sigma_{\mu\nu}\sigma^{\mu\nu} + \tilde{\omega}_{\mu\nu}\tilde{\omega}^{\mu\nu} - \boldsymbol{R}(\boldsymbol{\ell}, \boldsymbol{\ell}). \tag{1.4}$$

Shear-free, Twist-free congruence, assuming Null-Energy condition:

$$\frac{d\theta_{(\boldsymbol{\ell})}}{d\lambda} + \frac{1}{2}\theta_{(\boldsymbol{\ell})}^2 \leq 0, \tag{1.5}$$

Quasi-Local Framework

Trapped Surface

Future trapped surface

Compact cross-section $\mathscr{N}$, containing two systems of null geodesics, $\boldsymbol{\ell}$, $\boldsymbol{n}$, emerging orthogonally from $\mathscr{N}$, towards the future which converge locally, such that they have negative expansions

$$\theta_{(\boldsymbol{\ell})} < 0, \quad \theta_{(\boldsymbol{n})} < 0. \tag{1.6}$$

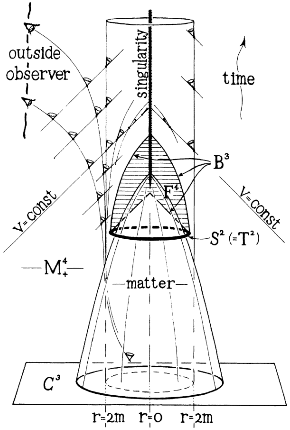

Phys. Rev. Lett. 14, 57.

Quasi-Equilibrium cases

Non-Expanding Horizons (NEH)

Null hypersurface $\mathscr{H}$, with topology $\mathscr{H} \simeq \mathbb{R} \times \mathscr{N}$, where $\mathscr{N}$ is a closed submanifold, such that the expansion of $\mathscr{H}$, along any null normal $\boldsymbol{\ell}$ vanishes identically.

All cross sections $\mathscr{N}$ of $\mathscr{H}$ have to be *Marginally Outer Trapped Surfaces.* Additionally, null energy condition, $T(\boldsymbol{\ell}, \boldsymbol{\ell}) \geq 0$, for any future-directed null normal $\boldsymbol{\ell}$.

Weakly Isolated Horizons

Weakly Isolated Horizon (WIH)

$(\mathscr{H}, [\ell])$ comprises a *weakly isolated horizon (WIH)*, if $\mathscr{H}$ is a NEH, and for each null normal ℓ in the equivalence class $[\ell]$, we have

$$^{\mathscr{H}}\mathcal{L}_{\ell}\omega_{\mathscr{H}} = 0, \tag{1.7}$$

Weakly Isolated Horizons

Lie derivative on the hypersurface:

$$\begin{aligned} {}^{\mathscr{H}}\mathcal{L}_{\boldsymbol{\ell}}\boldsymbol{\omega}_{\mathscr{H}} &= \boldsymbol{\ell}\cdot d\boldsymbol{\omega}_{\mathscr{H}} + d\boldsymbol{\omega}_{\mathscr{H}}(\boldsymbol{\ell})\Big|_{\mathscr{H}} \\ &= \boldsymbol{\ell}\cdot d\boldsymbol{\omega}_{\mathscr{H}} + \hat{\nabla}\kappa_{(\boldsymbol{\ell})} = 0. \end{aligned} \tag{1.8}$$

Using the intrinsic nature of the affine connection, $\hat{\nabla}\boldsymbol{\ell} = \boldsymbol{\ell}\otimes\boldsymbol{\omega}_{\mathscr{H}}$, we have:

$$\left[{}^{\mathscr{H}}\mathcal{L}_{\boldsymbol{\ell}}, \hat{\nabla}\right]\boldsymbol{\ell} = 0. \tag{1.9}$$

Isolated Horizons

Isolated Horizon

$(\mathscr{H}, [\ell])$ constitutes an *Isolated Horizon (IH)*, given $\mathscr{H}$ is a NEH, and each null normal ℓ in $[\ell]$ satisfies,

$$\left[{}^{\mathscr{H}}\mathcal{L}_{\ell}, \hat{\nabla} \right] = 0. \tag{1.10}$$

Beyond Equilibrium

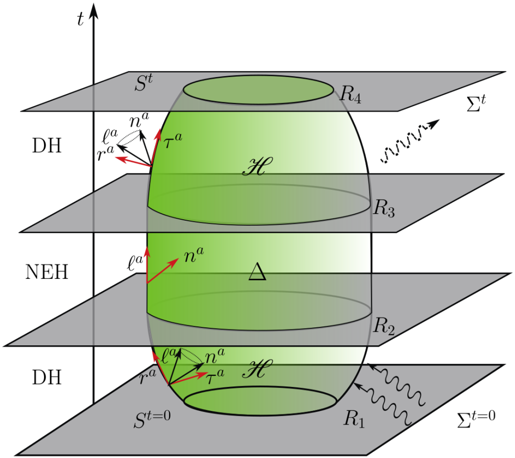

A. Ribes Metidieri. PhD thesis, Nijmegen U., 2025.

Near Horizon Spacetime

Characteristic Initial Value

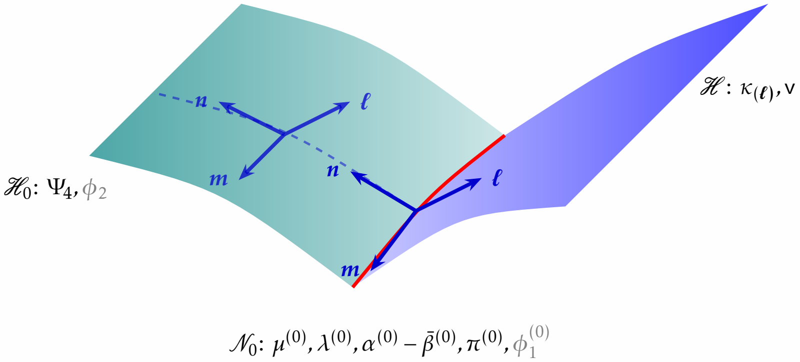

Frame Functions

Near-Horizon extension of local null tetrad,

$$\ell^i \nabla_i = D = \partial_{\mathsf{v}} + \mathsf{U}\partial_{\mathsf{r}} + \mathsf{X}^i \partial_{\mathsf{x}^i}\,, \tag{1.11a}$$

$$n^i \nabla_i = \Delta = -\partial_{\mathsf{r}}\,, \tag{1.11b}$$

$$m^i \nabla_i = \delta = \Omega \partial_{\mathsf{r}} + \xi^i \partial_{\mathsf{x}^i}\,. \tag{1.11c}$$

Horizon conditions: $\mathsf{U} \doteq 0$, $\mathsf{X}^i \doteq 0$, $\Omega \doteq 0$.

Near-Horizon Framework

Hamiltonian Calculations
Mass M, Surface gravity κ

Initial Data, Gauge Constraints
NEH/WIH, Rotation 1-form, Geodesic Nature

Multipole Moments, Algebraic Weyl properties
Intrinsic Geometry Characterization
Constraints on the Horizon

Newman-Penrose Field equations
Evolution & Constraint Equations
Radial Series Expansion

Spherical Background

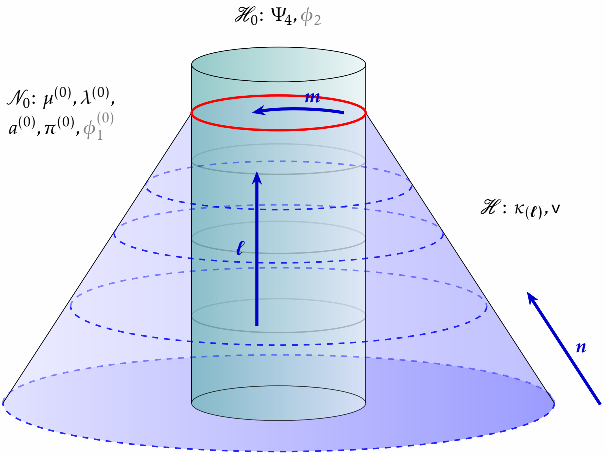

Tidal Deformations

Tidal Deformations

Astrophysical objects would deform when they are perturbed by external tidal fields quantified by the *Love numbers*.

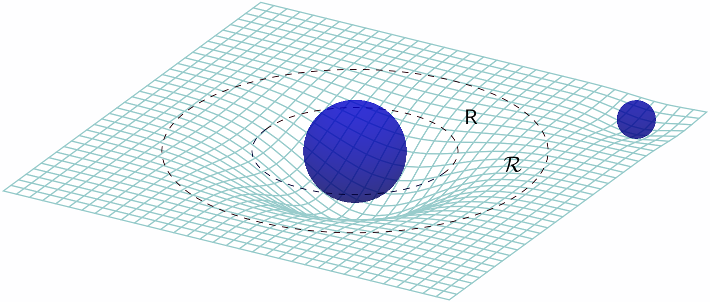

Newtonian Theory of Deformabilities

- Spherical Newtonian body of mass M and equilibrium radius R.
- Embedded in an external gravitational potential, $\Phi_{\text{ext}}(\mathsf{t}, \vec{\mathsf{x}})$.
- Symmetric, and trace-free tidal moments:

$$\mathcal{E}_L(\mathsf{t}) = -\frac{1}{(\ell - 2)!} \partial_{\langle L \rangle} \Phi_{\text{ext}}(\mathsf{t}, \vec{\mathsf{x}}_{\mathsf{COM}}). \tag{1.12}$$

for $0 \leq \mathsf{r} \leq \mathcal{R}$.

Deformed Gravitational Potential

Multipole moments of the deformed body, for $\mathsf{r} \geq \mathsf{R}$:

$$I_L(\mathsf{t}) = \int_{\mathbb{R}^3} d^3\mathsf{x}\ \delta\varrho(\mathsf{t}, \vec{\mathsf{x}})\mathsf{x}^{\langle L\rangle}, \tag{1.13}$$

where $\delta\varrho(\mathsf{t}, \vec{\mathsf{x}})$ is the mass density perturbation induced by the applied tidal field.

Total Gravitational Potential

Total Response:

$$\Phi(\mathsf{t},\vec{\mathsf{x}}) = -\sum_{\ell=2}^{\infty}\frac{1}{\ell(\ell-1)}\mathsf{x}^{L}\mathcal{E}_{L}(\mathsf{t}) + \frac{\mathsf{M}}{\mathsf{r}} + \sum_{\ell=2}^{\infty}\frac{(2\ell-1)!!}{\ell!}\frac{\mathsf{n}^{L}I_{L}(t)}{\mathsf{r}^{\ell+1}}, \tag{1.14}$$

with $\mathsf{r} = |\vec{\mathsf{x}}|$, and $\vec{\mathsf{n}} = \frac{1}{\mathsf{r}}\vec{\mathsf{x}}$.

Love Numbers

- Adiabatic approximation, Tidal deformability parameter:

$$I_L(\mathsf{t}) = -\lambda_\ell \mathcal{E}_L(\mathsf{t}), \tag{1.15}$$

  scales as $\mathsf{R}^{2\ell+1}$.

- Dimensionless tidal love numbers:

$$\lambda_\ell = \frac{2(\ell-2)!}{(2\ell-1)!!} k_\ell \mathsf{R}^{2\ell+1}, \tag{1.16}$$

- Potential:

$$\Phi(\mathsf{t},\mathsf{r},\xi,\bar{\xi}) = \frac{\mathsf{M}}{\mathsf{r}} - \sum_{\ell,m} \frac{1}{\ell(\ell-1)} \mathsf{r}^\ell \left[1 + 2k_\ell \left(\frac{\mathsf{R}}{\mathsf{r}}\right)^{2\ell+1}\right] \mathcal{E}_{\ell,m}(\mathsf{t}) Y_{\ell,m}(\xi,\bar{\xi}). \tag{1.17}$$

Relativistic Theory of Deformabilities

$$g_{00} = -1 + \frac{2\Phi}{c^2} + \mathcal{O}(c^{-4}), \tag{1.18a}$$

$$g_{0\mathrm{i}} = \mathcal{O}(c^{-3}), \tag{1.18b}$$

$$g_{\mathrm{ij}} = \delta_{\mathrm{ij}} \left(1 + \frac{2\Phi}{c^2}\right) + \mathcal{O}(c^{-4}). \tag{1.18c}$$

Relativistic Correspondence

Gauge-invariant formulation of the perturbed Coulombic potential:

$$\begin{aligned}\lim_{c\to\infty} c^2\Psi_2(\mathsf{t},\mathsf{r},\xi,\bar{\xi}) &= -\frac{1}{2}\frac{\partial}{\partial\mathsf{r}}^2\Phi(\mathsf{t},\mathsf{r},\xi,\bar{\xi}) \\ &= -\frac{\mathsf{M}}{\mathsf{r}^3} + \frac{1}{2}\sum_{\ell,m}\mathsf{r}^{\ell-2}\left[1+2\eta_\ell\left(\frac{\mathsf{R}}{\mathsf{r}}\right)^{2\ell+1}\right]\mathcal{E}_{\ell,m}(\mathsf{t})Y_{\ell,m}(\xi,\bar{\xi}) \qquad (1.19)\end{aligned}$$

where $\eta_\ell = \frac{(\ell+1)(\ell+2)}{\ell(\ell-1)}k_\ell$.

Surficial Love Numbers

- Deformation in Radius:

$$\hat{\mathsf{R}}(\mathsf{t},\xi,\bar{\xi}) = -\mathsf{R}\sum_{\ell,m}\frac{1}{\ell(\ell-1)}h_\ell\mathcal{E}_{\ell,m}(\mathsf{t})Y_{\ell,m}(\xi,\bar{\xi}), \tag{1.20}$$

where the surficial Love numbers h_ℓ are dimensionless.

- Curvature:

$$^{(2)}\hat{R}(\mathsf{t},\xi,\bar{\xi}) = -\frac{2}{\mathsf{R}^2}\sum_{\ell,m}\frac{\ell+2}{\ell}h_\ell\mathcal{E}_{\ell,m}(\mathsf{t})Y_{\ell,m}(\xi,\bar{\xi}). \tag{1.21}$$

Black Hole Perturbation Theory

Generic Cross-Section metric:

$$ds^2 \doteq \frac{2\mathsf{R}^2}{|P|^2} d\xi d\bar{\xi}. \tag{1.22}$$

Tidal Perturbation:

$$P \doteq P_{[0]} \left(1 + \hat{P}\right), \tag{1.23}$$

where $\hat{P}$ is a small perturbation, which we expand up to linear order.

Tidal Perturbations of Isolated Horizons

Perturbed Intrinsic Geometry:

$$ {}^{(2)}\hat{R} \doteq -4\Re\hat{\Psi}_2 \doteq 2\Delta_{[0]}\Re\hat{P} + 2\Re\hat{P}\,{}^{(2)}R_{[0]}. \tag{1.24}$$

where $\hat{\Psi}_2 \doteq \sum_{\ell,m} \hat{k}_{\ell,m} Y_{\ell,m}(\xi,\bar{\xi})$.

Teukolsky Equation

A seperable wave equation for the radiative Weyl scalar, $\hat{\Psi}_4$:

$$\mathcal{O}^{\Psi_4}_{[0]} \hat{\Psi}_4 = 0, \tag{1.25}$$

where $\mathcal{O}^{\Psi_4}_{[0]}$ is a background differential operator.

The Astrophysical Journal, **185**:635–647, 1973 October 15

PERTURBATIONS OF A ROTATING BLACK HOLE. I. FUNDAMENTAL EQUATIONS FOR GRAVITATIONAL, ELECTROMAGNETIC, AND NEUTRINO-FIELD PERTURBATIONS*

Saul A. Teukolsky†
California Institute of Technology, Pasadena
Received 1973 April 12

ABSTRACT

This paper derives linear equations that describe dynamical gravitational, electromagnetic, and neutrino-field perturbations of a rotating black hole. The equations decouple into a single gravitational equation, a single electromagnetic equation, and a single neutrino equation. Each of these equations is completely separable into ordinary differential equations. The paper lays the mathematical groundwork for later papers in this series, which will deal with astrophysical applications: stability of the hole, tidal friction effects, superradiant scattering of electromagnetic waves, and gravitational-wave processes.
Subject headings: black holes — gravitation — neutrinos — relativity — rotation

I. INTRODUCTION

This is the first in a series of papers which will deal with dynamical processes near a rotating black hole. The underlying mathematical technique throughout the series is to linearize the Einstein or Maxwell-Einstein equations around a known stationary black-hole solution, in this case the Kerr (1963) metric. This technique goes beyond previous work in which a rotating black hole has been treated as a fixed geometrical background for physical processes: the linearized equations give the hole the full dynamical freedom of small perturbations, including the possibility of gravitational and electromagnetic waves, secular changes in its mass and angular momentum, interaction with accreting test matter or distant massive objects, and so on.

The fundamental perturbation equations which will be used throughout the series are derived in this paper; in form, the equations are separable partial differential equations whose independent variables are certain decoupled components of the Weyl or Riemann tensor, or of the electromagnetic field tensor. Some of the applications to be treated in subsequent papers make direct use of only these decoupled components. Other applications require that one consider *all* components of the electromagnetic or gravitational field. Here, a concentration of attention on only the decoupled components would not *a priori* seem to be justified. However, for both gravitational and electromagnetic perturbations, it can be proved that the decoupled components contain complete information about all nontrivial features of the full perturbing field; this completeness will be discussed in a subsequent paper. For the electromagnetic case the result is due to Fackerell and Ipser (1972); for the gravitational case it is due to Wald (1973).

How does one obtain linearized perturbation equations, say for gravitational perturbations? A straightforward way is to start with the Einstein equations for a metric $g_{\mu\nu}$, and to let $g_{\mu\nu} = g_{\mu\nu}{}^A + h_{\mu\nu}{}^B$, where the superscripts A and B denote background and perturbation quantities, respectively. The field equations are then expanded to first order in $h_{\mu\nu}{}^B$, yielding a set of linear equations for the perturbations.

* Supported in part by the National Science Foundation [GP-36687X, GP-28027].
† United States Steel Foundation Fellow.

Teukolsky, Saul A., Astrophysical Journal, Vol. 185.

Gravitational Waves

Gravitational Wave Observations

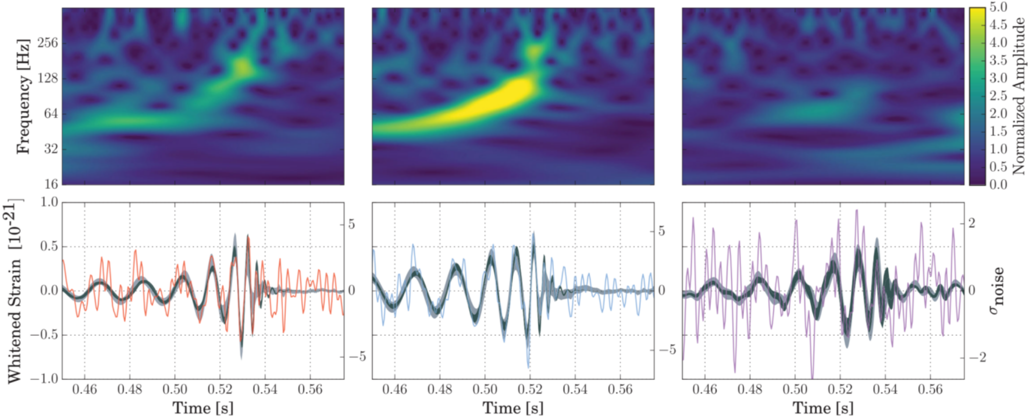

LVC Phys. Rev. Lett. 119, 141101.

Golden Era of Black Hole Astronomy

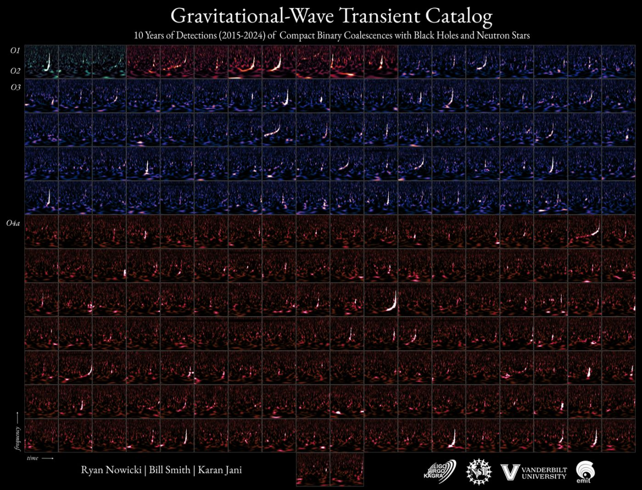

Ryan Nowicki / Bill Smith / Karan Jani

Waveform

Why Gravitational Waves?

Tests of General Relativity

- Provides direct access to the highly non-linear, strong-field regime of gravity.
- Allows us to observe the dynamical evolution of the spacetime fabric itself.

Astrophysical Implications

- Unveiling the mass and spin distributions of compact object populations to constrain stellar evolution models.
- Distinguishing between isolated binary evolution and dynamical formation mechanisms in dense stellar environments.

Why Gravitational Waves?

Searching for New Physics

- Distinguishing true black holes from exotic compact objects, and studying the nature of the remnant.
- Testing the *Kerr Hypothesis*, if the remnant's multipole moments uniquely match the Kerr metric via its quasi-normal modes.
- Probing for near-horizon quantum effects and potential theoretical echoes.

Binary Black Holes

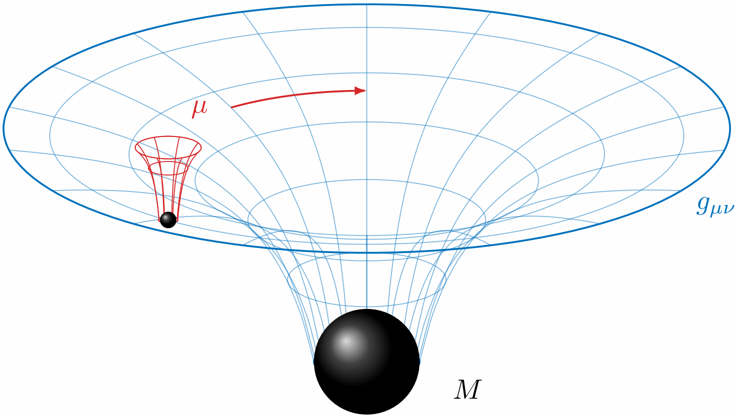

Linearized Gravity

Perturbations $h_{\mu\nu}$ over a flat background spacetime $\eta_{\mu\nu}$:

$$\boldsymbol{g} = \boldsymbol{\eta} + \boldsymbol{h}, \quad |h_{\mu\nu}| \ll 1. \tag{2.1}$$

In vacuum, applying the transverse-traceless (TT) gauge ($\partial^\mu h^{\mathrm{TT}}_{\mu\nu} = 0$, $\eta^{\mu\nu} h^{\mathrm{TT}}_{\mu\nu} = 0$):

$$\Box \bar{h}^{\mathrm{TT}}_{\mu\nu} = 0. \tag{2.2}$$

Physical radiative degrees of freedom are fully encoded in the two transverse polarization states, h_+ and $h_\times$

Newman-Penrose Connection

In our Newman-Penrose null tetrad, $\{\boldsymbol{\ell}, \boldsymbol{n}, \boldsymbol{m}, \bar{\boldsymbol{m}}\}$, the outgoing transverse radiation is isolated in the complex scalar Ψ_4:

$$\begin{aligned}\Psi_4 &= C_{\mu\nu\alpha\beta} n^\mu \bar{m}^\nu n^\alpha \bar{m}^\beta &(2.3)\\ &= \frac{1}{2}\left(\ddot{h}_+ - i\ddot{h}_\times\right) = \frac{1}{2}\ddot{h}. &(2.4)\end{aligned}$$

Proportional to the second time derivative of the complex gravitational wave strain $h = h_+ - ih_\times$.

Outlook

Fundamental Theory (Horizon Physics)

Testing the Kerr Hypothesis, Black Hole Spectroscopy.

Phenomenology (Waveforms)

Non-linearity, Astrophysical Models: Eccentricity, Spin-precession, Lensing.

Observation (Detectors, Data Analysis)

Confusion Noise, Overlapping Signals, Degeneracy Breaking.

Overlapping Gravitational Waves

Overlapping Transients

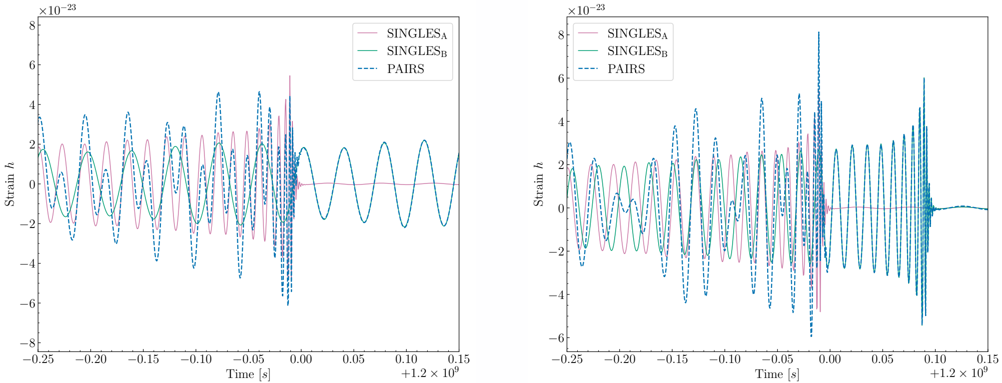

Degeneracy with Lensing

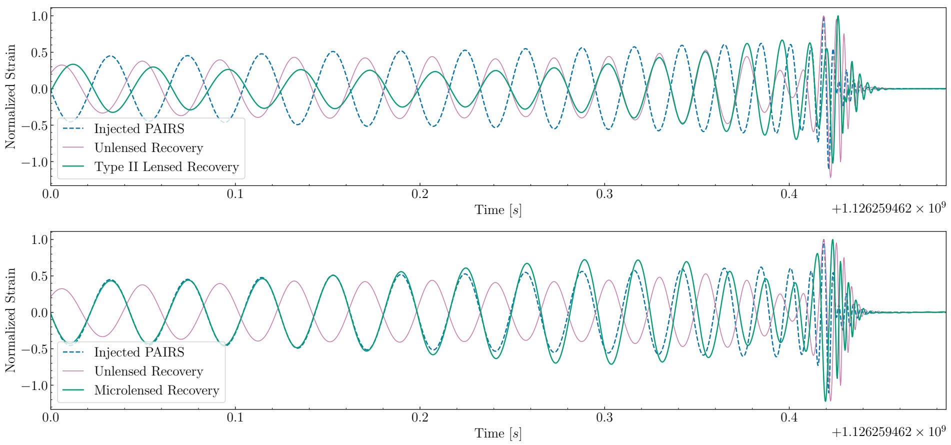

Analysis Techniques

Parameter Estimation

Bayesian inference:

$$\mathcal{L}(d|\theta) \propto \exp\left[-\frac{1}{2}\langle d - h(\theta)|d - h(\theta)\rangle\right] \tag{2.5}$$

$$\underbrace{\log_{10} \mathcal{B}_U^L}_{\text{Bayes Factor}} = \log_{10} \mathcal{Z}_L - \log_{10} \mathcal{Z}_U, \quad \mathcal{Z}_M = \int d\theta \mathcal{L}(d|\theta, \mathcal{H}_M)\pi_M(\theta|\mathcal{H}_M). \tag{2.6}$$

Analysis Techniques

Fitting Factor

Maximizing waveform overlap:

$$\mathcal{M}[h_1, h_2] = \max_{t_c, \Phi_c} \frac{\langle h_1 | h_2 \rangle}{\sqrt{\langle h_1 | h_1 \rangle \langle h_2 | h_2 \rangle}}. \tag{2.7}$$

$$\mathcal{F} = \max_{\lambda} \mathcal{M}[h_1, h_2(\lambda)], \quad \log_{10} \mathcal{B}_U^L = (\mathcal{F}_L^2 - \mathcal{F}_U^2) \frac{\mathrm{SNR}^2}{2}. \tag{2.8}$$

Study Overview

- Systematically vary key parameters influencing waveform evolution: Chirp mass ratio: $\mathscr{M}_{\mathrm{B}}/\mathscr{M}_{\mathrm{A}}$, SNR ratio: $\mathrm{SNR}_{\mathrm{B}}/\mathrm{SNR}_{\mathrm{A}}$, Coalescence time difference: Δt_c
- Inferences for **Unlensed** (single waveform), **Type II Lensed** (Strong Lensing, $n_j = 0.5$), **Microlensed** (Isolated point-mass lens), **Eccentricity** (Aligned spins) and **Spin-Precession**.

Study Details

Individual Case	Population Study
• $\mathscr{M}_{\rm B}/\mathscr{M}_{\rm A} \in \{0.5,\ 1,\ 2\}$ • $\mathrm{SNR_B}/\mathrm{SNR_A} \in \{0.5,\ 1\}$ • $\Delta t_c \in [-0.1,\ 0.1]$ s	• $\mathscr{M}_{\rm B}/\mathscr{M}_{\rm A} \in [0.1,\ 10]$ • $\mathrm{SNR_B}/\mathrm{SNR_A} \in [0.1,\ 10]$ • $\Delta t_c \in [-0.1,\ 0.1]$ s
Parameter Estimation (for 60 signals).	Fitting factor ($\sim \mathcal{O}(5000)$ signals).

Type II Lensed Parameter Estimation Inferences

$\mathcal{M}_B/\mathcal{M}_A \in \{0.5, 1, 2\},\ \mathrm{SNR_B}/\mathrm{SNR_A} \in \{0.5, 1\},\ \Delta t_c \in [-0.1, 0.1]s$

A : Fixed Morse phase shows distinct Bayes factor differences over the unlensed case.

B,C : Allowing the Morse phase to vary improves lensing characterization.

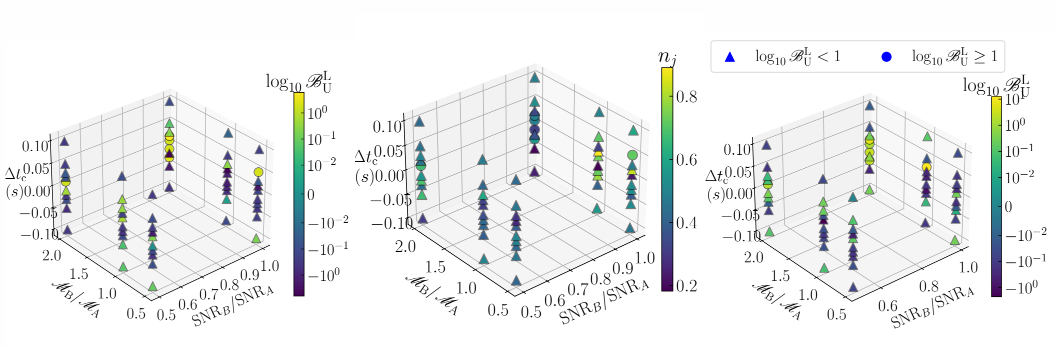

A B C

Microlensed Parameter Estimation Inferences

$\mathcal{M}_B/\mathcal{M}_A \in \{0.5, 1, 2\}$, $\mathrm{SNR_B}/\mathrm{SNR_A} \in \{0.5, 1\}$, $\Delta t_c \in [-0.1, 0.1]s$

- Microlensed templates yield stronger support for strongly overlapping signals.
- Maximally favored ($\log_{10} \mathscr{B}^{\mathrm{L}}_{\mathrm{U}} \gg 1$) for $\mathscr{M}_{\mathrm{B}}/\mathscr{M}_{\mathrm{A}} \gtrsim 1$ and equal SNRs, increasing with $|\Delta t_{\mathrm{c}}|$.

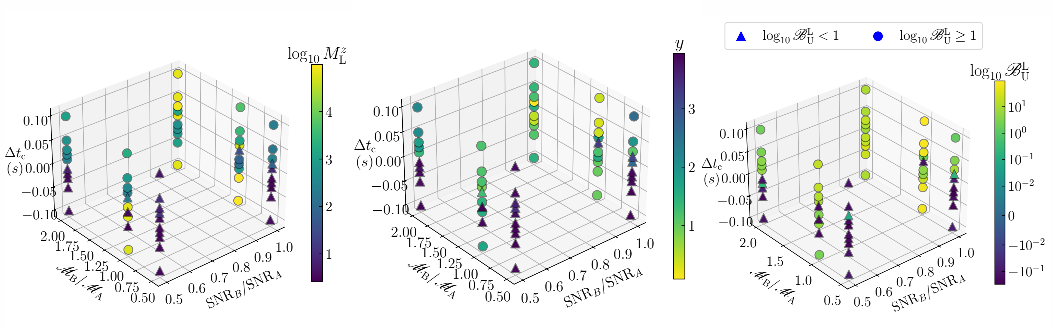

Microlensing Parameter Estimation Posteriors

$\mathcal{M}_B/\mathcal{M}_A \in \{0.5, 1, 2\}$, $\mathrm{SNR_B/SNR_A} \in \{0.5, 1\}$, $\Delta t_c \in [-0.1, 0.1]s$

- Inferred lens parameters (M_ℓ^z, y) show dependencies with $|\Delta t_c|$.
- The inferred redshifted lens masses lie in the range $M_\mathrm{L}^z \sim 10^2$–10^5 $\mathrm{M}_\odot$ with impact parameters $y \sim 0.1$–3.

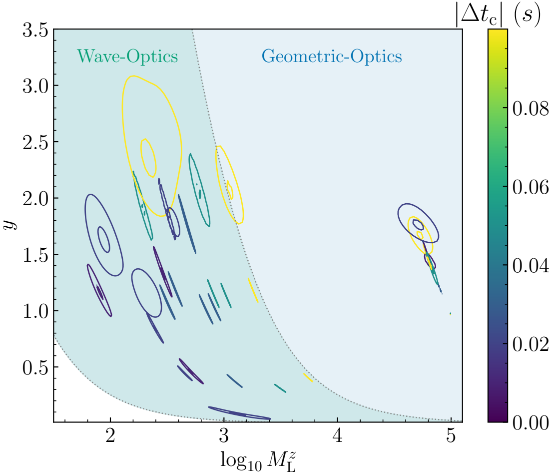

Microlensing Time Delay

$\mathcal{M}_B/\mathcal{M}_A \in \{0.5, 1, 2\},\ \mathrm{SNR_B/SNR_A} \in \{0.5, 1\},\ \Delta t_c \in [-0.1, 0.1]s$

- Inferred time delay of two superimposed microimages is close to the injected $|\Delta t_\mathrm{c}|$ or $(\delta - |\Delta t_\mathrm{c}|)$.
- False evidence for microlensing signatures, the model produces two superimposed images whose time delay can closely match $|\Delta t_\mathrm{c}|$.

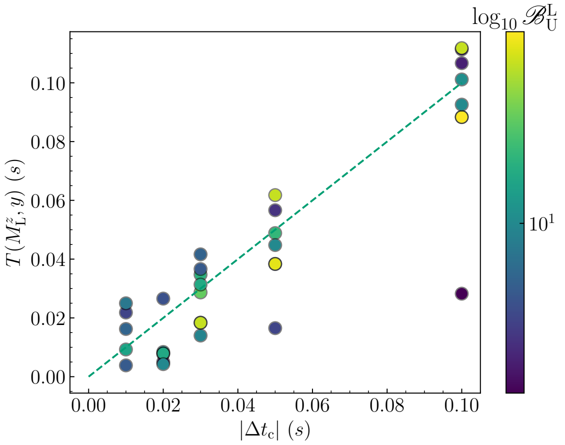

Eccentricity and Spin-Precession

$\mathcal{M}_B/\mathcal{M}_A \in \{0.5, 1, 2\}$, $\mathrm{SNR_B}/\mathrm{SNR_A} \in \{0.5, 1\}$, $\Delta t_c \in [-0.1, 0.1]s$

Support for Spin-Precession, $\chi_\mathrm{p} \gtrsim 0.5$ and $\chi_\mathrm{eff} \approx 0$. Minimal inference of orbital eccentricity, $e_0 \lesssim 0.1$.

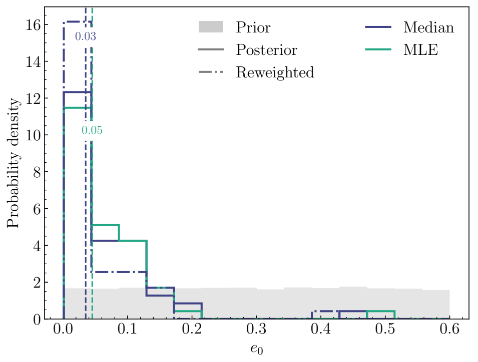

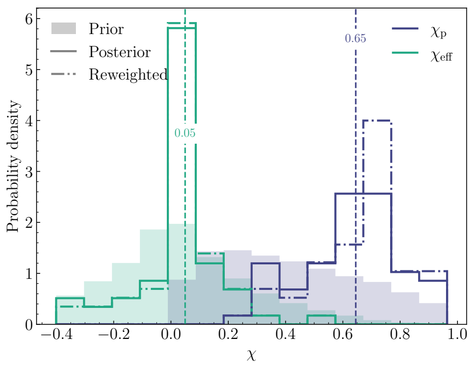

Ringdown Physics

Quasi-Normal Modes

Perturbed Kerr Black Hole, gravitational wave multipoles:

$$h_+ - ih_\times = -\frac{M}{r}\sum_{\ell,m,n}\mathcal{A}_{\ell,m,n}S(\theta,\varphi)e^{i\omega_{\ell,m,n}t}e^{-t/\tau_{\ell,m,n}} \tag{2.9}$$

Frequency $\omega_{\ell,m,n}$, Damping time $\tau_{\ell,m,n}$ predicted by Linear Perturbation theory, fixed by final mass, M, and spin, a. Amplitudes and relative phases predicted by numerical relativity.

Ringdown Observations

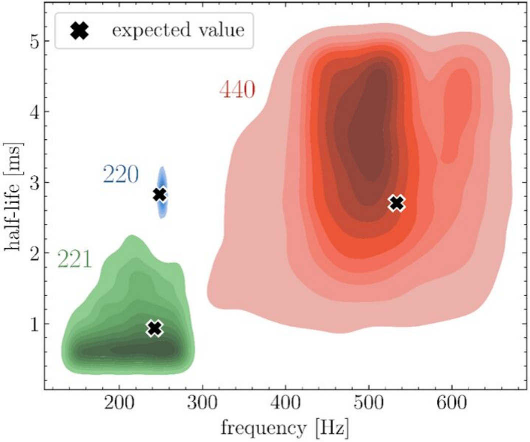

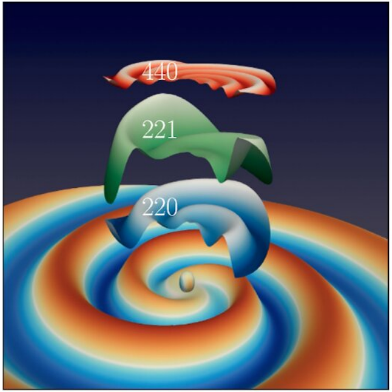

LVC Phys. Rev. Lett. 135, 111403.

Eccentricity

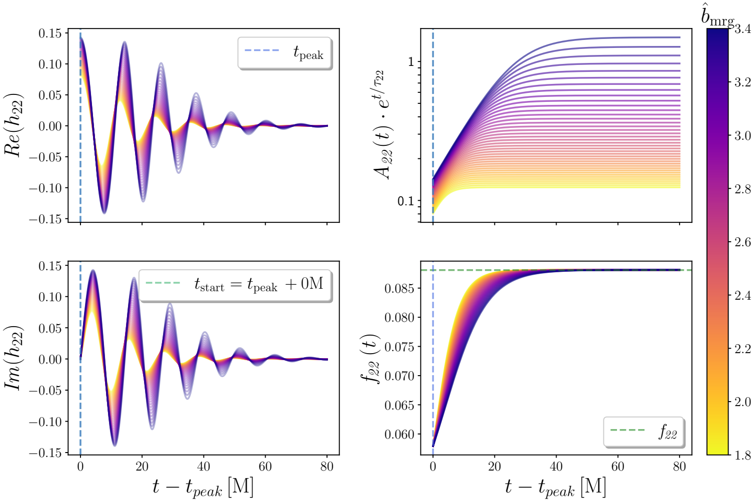

Analytic Representation

- Defining the QNM-rescaled waveform as $\bar{h}(\tau) = e^{\sigma_1 \tau + i\phi_{22}^{\text{mrg}}} h(\tau)$, where we factor out the contribution of the fundamental QNM $h_1(\tau) \sim e^{-\sigma_1 \tau}$ with $\sigma_1 = \alpha_1 + i\omega_1$, and ϕ_{22}^{mrg} being the value of ϕ_{22} at merger.
- Decomposing $\bar{h}(\tau) \equiv A_{\bar{h}}(\tau) e^{i\phi_{\bar{h}}(\tau)}$ with $\phi_{\bar{h}}(\tau) = \omega_1 \tau - \phi_{22}(\tau) + \phi_{22}^{\text{mrg}}$.

Analytic Representation

$$A_{\bar{h}}(\tau) = \left(\frac{c_1^A}{1 + \exp(-c_2^A \tau + c_3^A)} + c_4^A \right)^{\frac{1}{c_5^A}}$$

$$\phi_{\bar{h}}(\tau) = -c_1^\phi \ln \left(\frac{1 + c_3^\phi \exp(-c_2^\phi \tau) + c_4^\phi \exp(-2 c_2^\phi \tau)}{1 + c_3^\phi + c_4^\phi} \right)$$

- I $A_{\bar{h}}(\tau = 0) = A_{22}^{\text{mrg}}$ (NR).
- II $\left. \frac{dA_{\bar{h}}}{d\tau} \right|_{\tau=0} = \dot{A}_{22} \big|_{t=t_0}$.
- III $\left. \frac{d^2 A_{\bar{h}}}{d\tau^2} \right|_{\tau=0} = \ddot{A}_{22} \big|_{t=t_0}$.
- IV $\left. \frac{d\phi_{\bar{h}}}{d\tau} \right|_{\tau=0} = \Delta\omega = \omega_1 - \mathcal{M}_{\text{BH}} \omega_{22}^{\text{mrg}}$.

Analytic Representation

From the continuity conditions,

- $c_1^A = \frac{c_5^A \alpha_1}{c_2^A} (A_{22}^{\text{mrg}})^{c_5^A} \exp(-c_3^A)(1 + \exp(c_3^A))^2$ (from II)
- c_2^A *free parameter*
- c_3^A *free parameter*
- $c_4^A = (A_{22}^{\text{mrg}})^{c_5^A} - \frac{c_1^A}{1+\exp(c_3^A)}$ (from I)
- $c_5^A = -\frac{\ddot{A}_{22}^{\text{mrg}}}{A_{22}^{\text{mrg}} \alpha_1^2} + \frac{c_2^A}{\alpha_1} \frac{\exp(c_3^A)-1}{\exp(c_3^A)+1}$ (from IV)

- $c_1^\phi = \frac{1+c_3^\phi+c_4^\phi}{c_2^\phi(c_3^\phi+2c_4^\phi)} \Delta\omega$ (from IV)
- c_2^ϕ *free parameter*
- c_3^ϕ *free parameter*
- c_4^ϕ *free parameter*

Non-Linearity

Second-Order Perturbation Theory

$\boldsymbol{g} = \boldsymbol{g}_{[0]} + \epsilon \boldsymbol{h}^{(1)} + \epsilon^2 \boldsymbol{h}^{(2)}$, with linear homogeneous Teukolsky equation for the radiative Weyl scalar:

$$\mathcal{O}^{\Psi_4}_{[0]} \hat{\Psi}^{(1)}_4 = 0. \tag{2.10}$$

Second-order Weyl scalar, driven by a source term $\mathcal{S}$ constructed strictly from quadratic combinations of the first-order perturbations:

$$\mathcal{O}^{\Psi_4}_{[0]} \hat{\Psi}^{(2)}_4 = \mathcal{S}\left[\hat{\Psi}^{(1)}_4, \hat{\Psi}^{(1)}_4\right]. \tag{2.11}$$

Quadratic Mode Mixing

$$\omega_{\ell mn} = \omega_{\ell_1 m_1 n_1} + \omega_{\ell_2 m_2 n_2}, \tag{2.12a}$$

$$\frac{1}{\tau_{\ell mn}} = \frac{1}{\tau_{\ell_1 m_1 n_1}} + \frac{1}{\tau_{\ell_2 m_2 n_2}}, \tag{2.12b}$$

$$\mathcal{A}_{\ell mn} \propto \mathcal{A}_{\ell_1 m_1 n_1} \mathcal{A}_{\ell_2 m_2 n_2}. \tag{2.12c}$$

The Exciting Road Ahead

1. Mapping the tidal Love numbers and surficial horizon perturbations $\hat{\Psi}_2$ directly to my analytic ringdown observables extracted from $\hat{\Psi}_4$.
2. Extension of the study of overlapping gravitational wave transients against eccentricity and spin precession. Demonstrated that nearly equal chirp masses and comparable loud overlapping transients are degenerate with lensing effects.
3. Phenomenological fits for capturing eccentricity in Ringdown, study of non-linear modes in gravitational wave data.
4. Embedding quantum correlations in linearized gravity to uncover the Horizon structure.

Thanks!

References I

- Chandrasekhar, Subrahmanyan. *The mathematical theory of black holes.* Vol. 69. Oxford university press, 1998.
- Krishnan, Badri. *Quasi-local black hole horizons.* Springer Handbook of Spacetime, 2014: 527-555.
- Metidieri, Ariadna Ribes, Béatrice Bonga, and Badri Krishnan. *Tidal deformations of slowly spinning isolated horizons.* Physical Review D 110.2, 2024: 024069.
- Ashtekar, Abhay, Christopher Beetle, and Jerzy Lewandowski. *Geometry of generic isolated horizons.* Classical and Quantum Gravity 19.6: 1195.
- Krishnan, Badri. *The spacetime in the neighborhood of a general isolated black hole.* Classical and quantum gravity 29.20: 205006.
- Rao, N., Mishra, A., Ganguly, A. and More, A., 2026. *Comprehensive analysis of time-domain overlapping gravitational wave transients: A lensing study.* Physical Review D, 113(2), p.023054.
- Samajdar, A. et al., 2021. *Biases in parameter estimation from overlapping gravitational-wave signals in the third-generation detector era.* Physical Review D, 104(4), p.044003.

References II

- Relton, P. and Raymond, V., 2021. *Parameter estimation bias from overlapping binary black hole events in second generation interferometers*. Physical Review D, 104(8), p.084039.
- Nagar, Alessandro, et al. *Effective-one-body waveforms from dynamical captures in black hole binaries.* Physical Review D 103.6: 064013.
- Buonanno, Alessandra, and Thibault Damour. *Effective one-body approach to general relativistic two-body dynamics* Physical Review D 59.8: 084006.
- Damour, Thibault, and Alessandro Nagar. *New analytic representation of the ringdown waveform of coalescing spinning black hole binaries*. Physical Review D 90.2: 024054.
- Carullo, Gregorio. *Ringdown amplitudes of nonspinning eccentric binaries.* Journal of Cosmology and Astroparticle Physics 2024.10: 061.

Appendix

Isolated Black Hole Horizons

Spin Coefficients

Directional Derivatives: $D = \ell^\mu \nabla_\mu$, $\Delta = n^\mu \nabla_\mu$, $\delta = m^\mu \nabla_\mu$.

$$D\boldsymbol{\ell} = (\varepsilon + \bar{\varepsilon})\boldsymbol{\ell} - \bar{\kappa}\boldsymbol{m} - \kappa\bar{\boldsymbol{m}}, \tag{A.1a}$$

$$D\boldsymbol{n} = -(\epsilon + \bar{\epsilon})\boldsymbol{n} + \pi\boldsymbol{m} + \bar{\pi}\bar{\boldsymbol{m}}, \tag{A.1b}$$

$$D\boldsymbol{m} = \bar{\pi}\boldsymbol{\ell} - \kappa\boldsymbol{n} + (\epsilon - \bar{\epsilon})\boldsymbol{m}, \tag{A.1c}$$

$$\Delta\boldsymbol{\ell} = (\gamma + \bar{\gamma})\boldsymbol{\ell} - \bar{\tau}\boldsymbol{m} - \tau\bar{\boldsymbol{m}}, \tag{A.1d}$$

$$\Delta\boldsymbol{n} = -(\gamma + \bar{\gamma})\boldsymbol{n} + \nu\boldsymbol{m} + \bar{\nu}\bar{\boldsymbol{m}}, \tag{A.1e}$$

$$\Delta\boldsymbol{m} = \bar{\nu}\boldsymbol{\ell} - \tau\boldsymbol{n} + (\gamma - \bar{\gamma})\boldsymbol{m}, \tag{A.1f}$$

$$\delta\boldsymbol{\ell} = (\bar{\alpha} + \beta)\boldsymbol{\ell} - \bar{\varrho}\boldsymbol{m} - \sigma\bar{\boldsymbol{m}} \tag{A.1g}$$

$$\delta\boldsymbol{n} = -(\bar{\alpha} + \beta)\boldsymbol{n} + \mu\boldsymbol{m} + \bar{\lambda}\bar{\boldsymbol{m}}, \tag{A.1h}$$

$$\delta\boldsymbol{m} = \bar{\lambda}\boldsymbol{\ell} - \sigma\boldsymbol{n} + (\beta - \bar{\alpha})\boldsymbol{m}, \tag{A.1i}$$

$$\bar{\delta}\boldsymbol{m} = \bar{\mu}\boldsymbol{\ell} - \varrho\boldsymbol{n} + (\alpha - \bar{\beta})\boldsymbol{m}. \tag{A.1j}$$

Weyl Tensor

$$\Psi_0 = C_{\mu\nu\alpha\beta}\ell^{\mu}m^{\nu}\ell^{\alpha}m^{\beta}, \tag{A.2a}$$

$$\Psi_1 = C_{\mu\nu\alpha\beta}\ell^{i}n^{\nu}\ell^{\alpha}m^{\beta}, \tag{A.2b}$$

$$\Psi_2 = C_{\mu\nu\alpha\beta}\ell^{\mu}m^{\nu}\bar{m}^{\alpha}n^{\beta}, \tag{A.2c}$$

$$\Psi_3 = C_{\mu\nu\alpha\beta}\ell^{i}n^{\nu}\bar{m}^{\alpha}n^{\beta}, \tag{A.2d}$$

$$\Psi_4 = C_{\mu\nu\alpha\beta}n^{\mu}\bar{m}^{\nu}n^{\alpha}\bar{m}^{\beta}. \tag{A.2e}$$

Curvature Projections

$$\Lambda = \frac{R}{24}, \tag{A.3a}$$

$$\Phi_{00} = \frac{1}{2} R_{\mu\nu} \ell^\mu \ell^\nu, \tag{A.3b}$$

$$\Phi_{11} = \frac{1}{4} R_{\mu\nu} (\ell^\mu n^\nu + m^\mu \bar{m}^\nu), \tag{A.3c}$$

$$\Phi_{22} = \frac{1}{2} R_{\mu\nu} n^\mu n^\nu, \tag{A.3d}$$

$$\Phi_{01} = \frac{1}{2} R_{\mu\nu} \ell^\mu m^\nu, \tag{A.3e}$$

$$\Phi_{10} = \bar{\Phi}_{01} = \frac{1}{2} R_{\mu\nu} \ell^\mu \bar{m}^\nu, \tag{A.3f}$$

$$\Phi_{02} = \frac{1}{2} R_{\mu\nu} m^\mu m^\nu, \tag{A.3g}$$

$$\Phi_{20} = \bar{\Phi}_{02} = \frac{1}{2} R_{\mu\nu} \bar{m}^\mu \bar{m}^\nu, \tag{A.3h}$$

$$\Phi_{12} = \frac{1}{2} R_{\mu\nu} n^\mu m^\nu, \tag{A.3i}$$

$$\Phi_{21} = \frac{1}{2} R_{\mu\nu} n^\mu \bar{m}^\nu. \tag{A.3j}$$

Radial Field Equations

$$\Delta\pi - D\nu = -\mu\left(\pi + \bar{\tau}\right) - \lambda\left(\bar{\pi} + \tau\right) - \pi\left(\gamma - \bar{\gamma}\right) + \nu\left(3\epsilon + \bar{\epsilon}\right) - \Psi_3 - \Phi_{21}, \tag{A.4a}$$

$$\Delta\beta - \delta\gamma = \gamma\left(\bar{\alpha} + \beta - \tau\right) - \mu\tau + \sigma\nu + \epsilon\bar{\nu} + \beta\left(\gamma - \bar{\gamma} - \mu\right) - \alpha\bar{\lambda} - \Phi_{12}, \tag{A.4b}$$

$$\Delta\alpha - \bar{\delta}\gamma = \nu\left(\varrho + \epsilon\right) - \lambda\left(\tau + \beta\right) + \alpha\left(\bar{\gamma} - \bar{\mu}\right) + \gamma\left(\bar{\beta} - \bar{\tau}\right) - \Psi_3, \tag{A.4c}$$

$$\Delta\lambda - \bar{\delta}\nu = \lambda\left(\bar{\gamma} - 3\gamma - \mu - \bar{\mu}\right) + \nu\left(3\alpha + \bar{\beta} + \pi - \bar{\tau}\right) - \Psi_4, \tag{A.4d}$$

$$\Delta\mu - \delta\nu = -\mu^2 - |\lambda|^2 - \mu\left(\gamma + \bar{\gamma}\right) + \bar{\nu}\pi + \nu\left(\bar{\alpha} + 3\beta - \tau\right) - \Phi_{22}, \tag{A.4e}$$

$$\Delta\varrho - \bar{\delta}\tau = -\varrho\bar{\mu} - \sigma\lambda + \tau\left(\bar{\beta} - \alpha - \bar{\tau}\right) + \varrho\left(\gamma + \bar{\gamma}\right) + \nu\kappa - \Psi_2 - 2\Lambda, \tag{A.4f}$$

$$\Delta\sigma - \delta\tau = -\mu\sigma - \bar{\lambda}\varrho + \tau\left(\tau + \beta - \bar{\alpha}\right) + \sigma\left(3\gamma - \bar{\gamma}\right) + \kappa\bar{\nu} - \Phi_{02}, \tag{A.4g}$$

$$\Delta\kappa - D\tau = -\varrho\left(\tau + \bar{\pi}\right) - \sigma\left(\bar{\tau} + \pi\right) - \tau\left(\epsilon - \bar{\epsilon}\right) + \kappa\left(3\gamma + \bar{\gamma}\right) - \Psi_1 - \Phi_{01}, \tag{A.4h}$$

$$\Delta\epsilon - D\gamma = -\alpha\left(\tau + \bar{\pi}\right) - \beta\left(\bar{\tau} + \pi\right) + 2\gamma\epsilon + \gamma\bar{\epsilon} + \epsilon\bar{\gamma} - \tau\pi + \nu\kappa - \Psi_2 - \Phi_{11} + \Lambda, \tag{A.4i}$$

Evolution Field Equations

$$D\varrho - \bar{\delta}\kappa = \varrho^2 + |\sigma|^2 + \varrho\left(\epsilon + \bar{\epsilon}\right) - \bar{\kappa}\tau + \kappa\left(\pi - 3\alpha - \bar{\beta}\right) + \Phi_{00}, \tag{A.5a}$$

$$D\sigma - \delta\kappa = \sigma\left(3\epsilon - \bar{\epsilon} + \varrho + \bar{\varrho}\right) - \kappa\left(\bar{\pi} + \tau + 3\bar{\beta} + \alpha\right) + \Psi_0, \tag{A.5b}$$

$$D\alpha - \bar{\delta}\epsilon = \alpha\left(\varrho + \bar{\epsilon} - 2\epsilon\right) + \beta\bar{\sigma} - \bar{\beta}\epsilon - \kappa\lambda - \bar{\kappa}\gamma + \pi\left(\epsilon + \varrho\right) + \Phi_{10}, \tag{A.5c}$$

$$D\beta - \delta\epsilon = \sigma\left(\alpha + \pi\right) + \beta\left(\bar{\varrho} - \bar{\epsilon}\right) - \kappa\left(\mu + \gamma\right) + \epsilon\left(\bar{\pi} - \bar{\alpha}\right) + \Psi_1, \tag{A.5d}$$

$$D\lambda - \bar{\delta}\pi = \varrho\lambda + \bar{\sigma}\mu + \pi\left(\pi + \alpha - \bar{\beta}\right) - \nu\bar{\kappa} + \lambda\left(\bar{\epsilon} - 3\epsilon\right) + \Phi_{20}, \tag{A.5e}$$

$$D\mu - \delta\pi = \bar{\varrho}\mu + \sigma\lambda + \pi\left(\bar{\pi} - \bar{\alpha} + \beta\right) - \mu\left(\epsilon + \bar{\epsilon}\right) - \nu\kappa + \Psi_2 + 2\Lambda, \tag{A.5f}$$

Angular Field Equations

$$\delta\alpha - \bar{\delta}\beta = \mu\varrho - \lambda\sigma + |\alpha|^2 + |\beta|^2 - 2\alpha\beta + \gamma\left(\varrho - \bar{\varrho}\right) + \epsilon\left(\mu - \bar{\mu}\right) - \Psi_2 + \Phi_{11} + \Lambda, \tag{A.6a}$$

$$\delta\varrho - \bar{\delta}\sigma = \varrho\left(\bar{\alpha} + \beta\right) + \sigma\left(\bar{\beta} - 3\alpha\right) + \tau\left(\varrho - \bar{\varrho}\right) + \kappa\left(\mu - \bar{\mu}\right) - \Psi_1 + \Phi_{01}, \tag{A.6b}$$

$$\delta\lambda - \bar{\delta}\mu = \nu\left(\varrho - \bar{\varrho}\right) + \pi\left(\mu - \bar{\mu}\right) + \mu\left(\alpha + \bar{\beta}\right) + \lambda\left(\bar{\alpha} - 3\beta\right) - \Psi_3 + \Phi_{21}. \tag{A.6c}$$

Bianchi Identities I

$$
\begin{aligned}
D\Psi_2 - \bar{\delta}\Psi_1 - \bar{\delta}\Phi_{01} + \Delta\Phi_{00} = {} & -\lambda\Psi_0 + 2\Psi_1\left(\pi - \alpha\right) + 3\varrho\Psi_2 - 2\kappa\Psi_3 - 2\Phi_{01}\left(\alpha + \bar{\tau}\right) \\
& + 2\varrho\Phi_{11} + \bar{\sigma}\Phi_{02} - \Phi_{00}\left(\bar{\mu} - 2\gamma - 2\bar{\gamma}\right) - 2\tau\Phi_{10} \\
& - 2D\Lambda, \qquad \text{(A.7a)} \\
\bar{\delta}\Psi_2 - D\Psi_3 - \delta\Phi_{20} + D\Phi_{21} = {} & 2\lambda\Psi_1 - 3\pi\Psi_2 + 2\Psi_3\left(\epsilon - \varrho\right) + \kappa\Psi_4 + 2\Phi_{21}\left(\bar{\varrho} - \epsilon\right) \\
& - 2\mu\Phi_{10} + 2\pi\Phi_{11} - \bar{\kappa}\Phi_{22} - \Phi_{20}\left(2\bar{\alpha} - 2\beta - \bar{\pi}\right) \\
& - 2\bar{\delta}\Lambda, \qquad \text{(A.7b)} \\
\Delta\Psi_1 - \delta\Psi_2 + \bar{\delta}\Phi_{02} - \Delta\Phi_{01} = {} & \nu\Psi_0 + 2\Psi_1\left(\gamma - \mu\right) - 3\tau\Psi_2 + 2\sigma\Psi_3 + 2\Phi_{01}\left(\bar{\mu} - \gamma\right) \\
& - 2\varrho\Phi_{12} - \bar{\nu}\Phi_{00} + 2\tau\Phi_{11} + \Phi_{02}\left(\bar{\tau} - 2\bar{\beta} + 2\alpha\right) \\
& + 2\delta\Lambda, \qquad \text{(A.7c)} \\
\bar{\delta}\Psi_0 - D\Psi_1 - \delta\Phi_{00} + D\Phi_{01} = {} & \Psi_0\left(4\alpha - \pi\right) - 2\Psi_1\left(2\varrho + \epsilon\right) + 3\kappa\Psi_2 + 2\Phi_{01}\left(\epsilon + \bar{\varrho}\right)
\end{aligned}
$$

Bianchi Identities II

$$
\begin{aligned}
&+ 2\sigma\Phi_{10} - 2\kappa\Phi_{11} - \bar{\kappa}\Phi_{02}, && \text{(A.7d)}\\
\Delta\Psi_2 - \delta\Psi_3 + D\Phi_{22} - \delta\Phi_{21} &= 2\nu\Psi_1 - 3\mu\Psi_2 + 2\Psi_3\left(\beta - \tau\right) + \sigma\Psi_4 + 2\Phi_{21}\left(\bar{\pi} + \beta\right)\\
&- 2\mu\Phi_{11} - \bar{\lambda}\Phi_{20} + 2\pi\Phi_{12} + \Phi_{22}\left(\bar{\varrho} - 2\epsilon - 2\bar{\epsilon}\right)\\
&- 2\Delta\Lambda, && \text{(A.7e)}\\
D\Psi_4 - \bar{\delta}\Psi_3 - \bar{\delta}\Phi_{21} + \Delta\Phi_{20} &= -3\lambda\Psi_2 + 2\Psi_3\left(2\pi + \alpha\right) - \Psi_4\left(4\epsilon - \varrho\right) + 2\Phi_{21}\left(\alpha - \bar{\tau}\right)\\
&+ 2\nu\Phi_{10} + \bar{\sigma}\Phi_{22} - 2\lambda\Phi_{11} - \Phi_{20}\left(\bar{\mu} + 2\gamma - 2\bar{\gamma}\right), && \text{(A.7f)}\\
\Delta\Psi_0 - \delta\Psi_1 - \delta\Phi_{01} + D\Phi_{02} &= \Psi_0\left(4\gamma - \mu\right) - 2\Psi_1\left(2\tau + \beta\right) + 3\sigma\Psi_2 + 2\Phi_{01}\left(\bar{\pi} - \beta\right)\\
&- 2\kappa\Phi_{12} - \bar{\lambda}\Phi_{00} + 2\sigma\Phi_{11} + \Phi_{02}\left(\bar{\varrho} + 2\epsilon - 2\bar{\epsilon}\right), && \text{(A.7g)}\\
\Delta\Psi_3 - \delta\Psi_4 - \Delta\Phi_{21} + \bar{\delta}\Phi_{22} &= 3\nu\Psi_2 - 2\Psi_3\left(\gamma + 2\mu\right) - \Psi_4\left(\tau - 4\beta\right) + 2\Phi_{21}\left(\bar{\mu} + \gamma\right)\\
&- 2\nu\Phi_{11} - \bar{\nu}\Phi_{20} + 2\lambda\Phi_{12} + \Phi_{22}\left(\bar{\tau} - 2\alpha - 2\bar{\beta}\right), && \text{(A.7h)}
\end{aligned}
$$

Maxwell's Equations

Field Projections,

$$\phi_0 = F_{\mu\nu}\ell^\mu m^\nu, \quad \phi_1 = \frac{1}{2}F_{\mu\nu}\left(\ell^\mu n^\nu + \bar{m}^\mu m^\nu\right), \quad \phi_2 = F_{\mu\nu}\bar{m}^\mu n^\nu, \tag{A.8}$$

Field Equations,

$$D\phi_1 - \bar{\delta}\phi_0 = \phi_0\left(\pi - 2\alpha\right) + 2\varrho\phi_1 - \kappa\phi_2 + 2\pi J_\ell, \tag{A.9a}$$

$$\delta\phi_2 - \Delta\phi_1 = \phi_2\left(\tau - 2\beta\right) - \nu\phi_0 + 2\mu\phi_1 + 2\pi J_n, \tag{A.9b}$$

$$\delta\phi_1 - \Delta\phi_0 = \phi_0\left(\mu - 2\gamma\right) + 2\tau\phi_1 - \sigma\phi_2 + 2\pi J_m, \tag{A.9c}$$

$$D\phi_2 - \bar{\delta}\phi_1 = \phi_2\left(\varrho - 2\epsilon\right) - \lambda\phi_0 + 2\pi\phi_1 + 2\pi J_{\bar{m}}. \tag{A.9d}$$

Field Tensor, $\Phi_{\mu\nu} = 2\phi_\mu\bar{\phi}_\nu$

Null Hypersurfaces

- *First Fundamental Form* $\boldsymbol{q}$ is the pull-back of $\boldsymbol{g}$ onto the hypersurface $\mathscr{H}$:

$$\boldsymbol{q}(\boldsymbol{u},\boldsymbol{v}) = \boldsymbol{g}(\boldsymbol{u},\boldsymbol{v}), \quad \forall(\boldsymbol{u},\boldsymbol{v}) \in T_p\mathscr{H} \times T_p\mathscr{H}\,. \tag{A.10}$$

- Normal vectors $\boldsymbol{\ell}$ to $\mathscr{H}$ are null and tangent to null geodesics ruling $\mathscr{H}$:

$$\nabla_{\boldsymbol{\ell}}\boldsymbol{\ell} = \kappa_{(\boldsymbol{\ell})}\boldsymbol{\ell}. \tag{A.11}$$

Weingarten Map

- The Weingarten map χ defines the extrinsic curvature by capturing the variation of the normal $\boldsymbol{\ell}$

$$\boldsymbol{\chi}(\boldsymbol{v}) = \nabla_{\boldsymbol{v}} \boldsymbol{\ell}. \tag{A.12}$$

- *Second Fundamental Form* $\boldsymbol{\Theta}$:

$$\boldsymbol{\Theta}\left(\boldsymbol{u}, \boldsymbol{v}\right) = \boldsymbol{u} \cdot \boldsymbol{\chi}(\boldsymbol{v}) = \nabla \underline{\boldsymbol{\ell}}\left(\boldsymbol{u}, \boldsymbol{v}\right). \tag{A.13}$$

- Due to degeneracy, $\boldsymbol{\Theta}$ vanishes along the null direction $\boldsymbol{\ell}$:

$$\boldsymbol{\Theta}\left(\boldsymbol{\ell}, \boldsymbol{v}\right) = \kappa_{(\boldsymbol{\ell})} \boldsymbol{v} \cdot \boldsymbol{\ell} = 0. \tag{A.14}$$

Cross Section

- A cross section $\mathscr{N}$ is a codimension-2 spacelike submanifold. The induced metric $\boldsymbol{h}$ on $\mathscr{N}$ is positive definite:

$$\boldsymbol{h}(\boldsymbol{u},\boldsymbol{v}) = \boldsymbol{g}(\boldsymbol{u},\boldsymbol{v}), \quad \forall(\boldsymbol{u},\boldsymbol{v}) \in T_p\mathscr{N} \times T_p\mathscr{N}. \tag{A.15}$$

- The tangent space of $\mathscr{M}$ orthogonally decomposes into $T_p\mathscr{N}$ and its complement:

$$T_p\mathscr{M} = T_p\mathscr{N} \oplus T_p^{\perp}\mathscr{N}. \tag{A.16}$$

- We choose a transverse future-directed null vector $\boldsymbol{n}$:

$$\boldsymbol{\ell}\cdot\boldsymbol{n} = -1, \quad T_p^{\perp}\mathscr{N} = \mathrm{Span}(\boldsymbol{\ell},\boldsymbol{n}). \tag{A.17}$$

Geodesic Kinematics

- Extending the second fundamental form via projection gives the generalized deformation tensor $\boldsymbol{\Theta}$:

$$\boldsymbol{\Theta}(\boldsymbol{u}, \boldsymbol{v}) = \nabla \underline{\boldsymbol{\ell}} \left(\vec{\boldsymbol{q}}(\boldsymbol{u}), \vec{\boldsymbol{q}}(\boldsymbol{v}) \right) . \tag{A.18}$$

- The full spacetime covariant derivative of the null normal expands to:

$$\nabla \underline{\boldsymbol{\ell}} = \boldsymbol{\Theta} + \underline{\boldsymbol{\ell}} \otimes \boldsymbol{\omega} - \nabla_{\boldsymbol{n}} \underline{\boldsymbol{\ell}} \otimes \underline{\boldsymbol{\ell}}. \tag{A.19}$$

- The rotation 1-form $\boldsymbol{\omega}$ handles the transverse variation:

$$\boldsymbol{\omega}(\boldsymbol{v}) = -\boldsymbol{n} \cdot \boldsymbol{\chi}(\boldsymbol{v}) = -\boldsymbol{n} \cdot \nabla_{\boldsymbol{\Pi}(\boldsymbol{v})} \boldsymbol{\ell}. \tag{A.20}$$

Cauchy Initial Value Problem

3+1 Decomposition

$\mathscr{M}$ is foliated into spacelike Cauchy slices Σ_t. The coordinate time vector decomposes using the lapse N and shift vector $\boldsymbol{N}$:

$$\boldsymbol{\partial}_t = N\boldsymbol{n} + \boldsymbol{N}. \tag{A.21}$$

The spatial metric $\boldsymbol{q}$ acts as the initial data coordinate system:

$$ds^2 = -N^2 dt^2 + q_{ij}\left(dx^i + N^i dt\right)\left(dx^j + N^j dt\right). \tag{A.22}$$

Initial Value: Constraints and Evolution

- The *extrinsic curvature* $\boldsymbol{K}$ describes the embedding of Σ_t in $\mathscr{M}$:

$$\boldsymbol{K} = -\nabla \underline{\boldsymbol{n}} - \boldsymbol{D} \ln N \otimes \underline{\boldsymbol{n}}. \tag{A.23}$$

- *Hamiltonian* and *Momentum* constraints restrict initial data on Σ_t:

$$\begin{aligned} {}^{(3)}R + K^2 - K_{\mu\nu}K^{\mu\nu} &= 16\pi E, \\ D^\mu K_{\alpha\mu} - D_\alpha K &= 8\pi J_\alpha. \end{aligned} \tag{A.24}$$

- Evolution of the spatial metric is governed by the Lie derivative:

$$\mathcal{L}_{N\boldsymbol{n}} q_{\mu\nu} = -2NK_{\mu\nu}. \tag{A.25}$$

Near Horizon Spin Coefficients

$\boldsymbol{n}$ affinely paramterized, and $\boldsymbol{\ell}$, $\boldsymbol{m}$ are parallel propagated along $\boldsymbol{n}$,

$$\tau = \nu = \gamma = 0. \tag{A.26}$$

Commutation Relations,

$$\mu = \bar{\mu}, \quad \pi = \alpha + \bar{\beta}. \tag{A.27}$$

Geodesic, hypersurface-orthogonal and expansion-free nature of $\boldsymbol{\ell}$,

$$\kappa \doteq \varrho \doteq 0, \tag{A.28}$$

Raychaudhuri's Equation constrains the shear-free nature,

$$\sigma \doteq 0. \tag{A.29}$$

Near Horizon Field Equations

Time evolution equations containing the directional derivative D,

$$D\varrho - \bar{\delta}\kappa = \varrho^2 + |\sigma|^2 + \varrho(\epsilon + \bar{\epsilon}) - 2\kappa\alpha, \quad \text{(A.30a)}$$

$$D\sigma - \delta\kappa = \sigma(\epsilon + \bar{\epsilon} + \varrho + \bar{\varrho}) - 2\kappa\beta + \Psi_0, \quad \text{(A.30b)}$$

$$D\alpha - \bar{\delta}\epsilon = \alpha(\varrho + \bar{\epsilon} - 2\epsilon) + \beta\bar{\sigma} - \bar{\beta}\epsilon - \kappa\lambda + \pi(\epsilon + \varrho), \quad \text{(A.30c)}$$

$$D\beta - \delta\epsilon = \sigma(\alpha + \pi) + \beta(\bar{\varrho} - \bar{\epsilon}) - \kappa\mu + \epsilon(\bar{\pi} - \bar{\alpha}) + \Psi_1, \quad \text{(A.30d)}$$

$$D\lambda - \bar{\delta}\pi = \lambda(\varrho - 2\epsilon) + \bar{\sigma}\mu + 2\pi\alpha, \quad \text{(A.30e)}$$

$$D\mu - \delta\pi = \mu(\bar{\varrho} - \epsilon - \bar{\epsilon}) + \sigma\lambda + 2\pi\beta + \Psi_2, \quad \text{(A.30f)}$$

Angular Field Equations

$$\delta\alpha - \bar{\delta}\beta = \mu\varrho - \lambda\sigma + |\alpha|^2 + |\beta|^2 - 2\alpha\beta - \Psi_2, \tag{A.31a}$$

$$\delta\varrho - \bar{\delta}\sigma = \varrho\bar{\pi} + \sigma\left(\bar{\beta} - 3\alpha\right) - \Psi_1, \tag{A.31b}$$

$$\delta\lambda - \bar{\delta}\mu = \mu\pi + \lambda\left(\bar{\alpha} - 3\beta\right) - \Psi_3. \tag{A.31c}$$

Radial Field Equations *(Decoupled)*

$$\Delta\pi = -\mu\pi - \lambda\bar{\pi} - \Psi_3, \tag{A.32a}$$

$$\Delta\beta = -\beta\mu - \alpha\bar{\lambda}, \tag{A.32b}$$

$$\Delta\alpha = -\lambda\beta - \alpha\mu - \Psi_3, \tag{A.32c}$$

$$\Delta\lambda = -2\lambda\mu - \Psi_4, \tag{A.32d}$$

$$\Delta\mu = -\mu^2 - |\lambda|^2, \tag{A.32e}$$

$$\Delta\varrho = -\varrho\mu - \sigma\lambda - \Psi_2, \tag{A.32f}$$

$$\Delta\sigma = -\mu\sigma - \bar{\lambda}\varrho, \tag{A.32g}$$

$$\Delta\kappa = -\varrho\bar{\pi} - \sigma\pi - \Psi_1, \tag{A.32h}$$

$$\Delta\epsilon = -\alpha\bar{\pi} - \beta\pi - \Psi_2, \tag{A.32i}$$

Near Horizon Bianchi Identities

Evolution equations,

$$D\Psi_1 - \bar{\delta}\Psi_0 = \Psi_0\left(\pi - 4\alpha\right) + 2\Psi_1\left(2\varrho + \epsilon\right) - 3\kappa\Psi_2, \tag{A.33a}$$

$$D\Psi_2 - \bar{\delta}\Psi_1 = -\lambda\Psi_0 - 2\Psi_1\left(\pi - \alpha\right) + 3\varrho\Psi_2 - 2\kappa\Psi_3, \tag{A.33b}$$

$$D\Psi_3 - \bar{\delta}\Psi_2 = -2\lambda\Psi_1 + 3\pi\Psi_2 - 2\Psi_3\left(\epsilon - \varrho\right) - \kappa\Psi_4, \tag{A.33c}$$

$$D\Psi_4 - \bar{\delta}\Psi_3 = -3\lambda\Psi_2 + 2\Psi_3\left(2\pi + \alpha\right) - \Psi_4\left(4\epsilon - \varrho\right), \tag{A.33d}$$

Radial Bianchi Identities

$$\Delta\Psi_0 - \delta\Psi_1 = -\mu\Psi_0 - 2\beta\Psi_1 + 3\sigma\Psi_2, \tag{A.34a}$$

$$\Delta\Psi_1 - \delta\Psi_2 = -2\mu\Psi_1 + 2\sigma\Psi_3, \tag{A.34b}$$

$$\Delta\Psi_2 - \delta\Psi_3 = -3\mu\Psi_2 + 2\beta\Psi_3 + \sigma\Psi_4, \tag{A.34c}$$

$$\Delta\Psi_3 - \delta\Psi_4 = -4\mu\Psi_3 + 4\beta\Psi_4. \tag{A.34d}$$

Since no radial derivative component for Ψ_4, given as free data that we provide on the null hypersurface $\mathscr{H}_0$.

Gravitational Waves

Population Fitting Factor Results: Type II Lensed Template

- $\log_{10} \mathscr{B}^{\mathrm{L}}_{\mathrm{U}} > 1$ in a small region of the overlapping parameter space with $\mathscr{M}_{\mathrm{B}}/\mathscr{M}_{\mathrm{A}} \gtrsim 1$ and $|\Delta t_{\mathrm{c}}| \leq 0.03$ s.
- Inferred Morse index clustering near $n_j \simeq 0.5$, indicative of Type-II lensing, for the cumulative study.

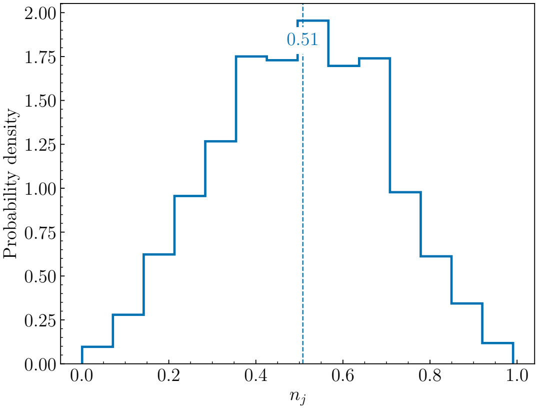

Population Fitting Factor Results: Microlensed Template

FF optimization shows moderate microlensing support when $\mathrm{SNR_B}/\mathrm{SNR_A} \sim 1$, consistent with PE trends.

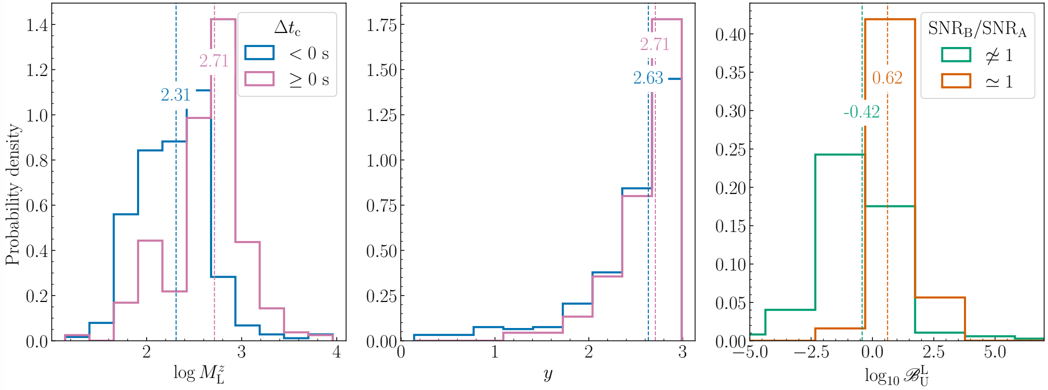

Newtonian Effective Potential

$$\tilde{V}_{\text{eff}} = -\frac{M}{r} + \frac{\tilde{l}^2}{r^2}$$

- Circular orbits at the global minimum, where $\frac{\partial \tilde{V}}{\partial r} = 0$.
- For bound orbits, $\tilde{E} < 0$ but larger than the minimum of the potential: elliptical with $r_{\pm} = -\frac{M}{2\tilde{E}}\left(1 \pm \sqrt{\frac{2\tilde{E}\tilde{l}^2}{M^2} + 1}\right)$.
- Parabolic for $\tilde{E} = 0$, Hyperbolic for $\tilde{E} > 0$.

Schwarzschild Effective Potential

$$\begin{aligned}\tilde{V}_{\text{eff}} &= -\frac{M}{r} + \frac{\tilde{l}^2}{r^2} - \frac{M\tilde{l}^2}{r^3} \\ &= -\frac{M}{r} + \frac{\tilde{l}^2}{2r^2}\left(1 - \frac{R_s}{r}\right)\end{aligned}$$

The additional term is negligible at large radii. Secondary extremum in potential.

EOB Framework

- Two-body dynamics $\to$ One-effective body in deformed spactime, parameter $\nu = \frac{\mu}{M} = \frac{m_1 m_2}{M^2}$.
- $H_{\text{Newt}} + \sum H_{\text{PN}} \to \mu \sqrt{A_\nu(r) \left[1 + \frac{p^2}{\mu^2} + \left(\frac{1}{B_\nu(r)} - 1\right)\right] \frac{p_r^2}{\mu^2}}$.
- $ds^2 = -A_\nu(r)dt^2 + B_\nu(r)dr^2 + r^2 d\Omega^2$.

EOB Framework

- EOB Hamiltonian $\hat{H} \equiv \frac{H}{\mu} = \frac{M}{\mu}\sqrt{1 + \frac{2\mu}{M}(H_{\text{eff}} - 1)}$. $H_{\text{eff}} = H_{\text{eff}}^{\text{orb}} + H_{\text{spin-oribt}}$ where $H_{\text{eff}}^{\text{orb}} = \sqrt{A\left(1 + \frac{p_\phi^2}{r_c^2} + Q\right) + p_{r_*}^2}$.
- Potential energy $E = M\sqrt{1 + \frac{2\mu}{M}(\hat{W}_{\text{eff}} - 1)}$ where $\hat{W}_{\text{eff}} = \sqrt{A(r)\left(1 + \frac{p_\phi^2}{r^2}\right)}$ defining stability at $\frac{\partial \hat{W}_{\text{eff}}}{\partial r} = \frac{\partial^2 \hat{W}_{\text{eff}}}{\partial r^2} = 0$.

EOB Parameterization

- Mass-normalized energy $h \equiv \frac{E}{M}$, and angular momentum $j \equiv \frac{J}{\nu M^2}$.
- EOB Effective energy $\hat{E}_{\text{eff}} = \frac{E_{\text{eff}}}{\mu} = 1 + \frac{h^2-1}{2\nu}$, and impact parameter $\hat{b}_{\text{EOB}} = \frac{b_{\text{EOB}}}{M} = \frac{jh}{\sqrt{\hat{E}_{\text{eff}}^2 - 1}}$. For bound configurations with $\hat{E}_{\text{eff}} < 1$, $\hat{b}_{\text{EOB}} = \frac{jh}{E_{\text{eff}}}$ at merger as dynamical impact parameter.

Quasi-Normal Modes

Exponentially decaying sinusoids given by

$$h_+ - ih_\times = \frac{1}{r}\sum_{\ell mn} \exp(i\omega_{\ell mn} t)\exp(-t/\tau) S_{\ell mn}(\iota, \beta) \mathcal{Z}^{\text{out}}_{\ell mn},$$

Factoring out $\mathcal{Z}^{\text{out}}_{\ell mn} = M\mathcal{A}_{\ell mn}\exp(i\Phi_{\ell mn})$, we have

$$h_+ - ih_\times = \frac{M}{r}\sum_{\ell mn} \mathcal{A}_{\ell mn}\exp(i\omega_{\ell mn} t + \Phi_{\ell mn})\exp(-t/\tau) S_{\ell mn}.$$

Ringdown Waveform model

Formally, Superposition of damped sinusoids and an exponentially decaying tail term.

$$h_{\ell m}(t) = \sum_{\ell' mn}^{\infty} \Big[A^{+}_{\ell n} \exp\{i(\omega^{+}_{\ell' mn}(t - t_{\text{ref}}) + \phi^{+}_{\ell' mn})\} + A^{-}_{\ell' mn} \exp\{i(\omega^{-}_{\ell' mn}(t - t_{\text{ref}}) + \phi^{-}_{\ell' mn})\} \Big] \theta(t - t^{\text{ref}}_{\text{start}}) + A^{T}_{\ell m} \exp\{i\phi^{T}_{\ell m}\}(t - t_{\text{ref}})^{p^{T}_{\ell m}} \theta(t - t^{\text{tail}}_{\text{start}}).$$

Effective Characterization

- Non-bijective amplitude dependence on eccentricity. Gauge-invariant parameterisation, shifting the perspective from orbital-based parameterisations to dynamics-based ones.
- Effective parameter space of quasi-universality through derived impact parameter at merger, the effective energy and the perturbation parameter of the metric $(\nu, \hat{b}_{\mathrm{mrg}}, E_{\mathrm{eff}}^{\mathrm{mrg}})$ for the global fit.

Ringdown Structure

- From initial $(E_0^{\text{ADM}}, J_0^{\text{ADM}})$, at time t, $(E(t), J(t))$, such that $E(t) = E_0^{\text{ADM}} - \int_{t_0}^{t} dt' \dot{E}(t')$ and $J(t) = J_0^{\text{ADM}} - \int_{t_0}^{t} dt' \dot{J}(t')$, where $\dot{E} = \frac{1}{16\pi} \sum_{\ell=2}^{\ell_{\max}} \sum_{m=-\ell}^{\ell} |\dot{h}_{\ell m}|^2$ and $\dot{J} = \frac{1}{16\pi} \sum_{\ell=2}^{\ell_{\max}} \sum_{m=-\ell}^{\ell} m \Im\{h_{\ell m} \dot{h}^*_{\ell m}\}$.
- Merger quantities at t_{mrg} corresponding to the peak of the emission immediately before a ringdown begins.

Analytic Representation

$$A_{\bar{h}}(\tau) = c_1^A \tanh(c_2^A \tau + c_3^A) + c_4^A$$
$$\phi_{\bar{h}}(\tau) = -c_1^\phi \ln\left(\frac{1 + c_3^\phi \exp(-c_2^\phi \tau) + c_4^\phi \exp(-2c_2^\phi \tau)}{1 + c_3^\phi + c_4^\phi}\right)$$

- I $A_{\bar{h}}(\tau = 0) = A_{22}^{\text{mrg}}$ (NR).
- II $\left.\frac{dA_{\bar{h}}}{d\tau}\right|_{\tau=0} = \dot{A}_{22}\big|_{t=t_0}$.
- III $c_2^A = \frac{\alpha_2 - \alpha_1}{2}$.
- IV $\left.\frac{d\phi_{\bar{h}}}{d\tau}\right|_{\tau=0} = \Delta\omega = \omega_1 - \mathcal{M}_{\text{BH}}\omega_{22}^{\text{mrg}}$.
- V $c_2^\phi = \alpha_2 - \alpha_1$.

Analytic Representation

From the continuity conditions,

- $c_1^A = A_{22}^{\mathrm{mrg}} \alpha_1 \frac{\cosh^2 c_3^A}{c_2^A}$ (from II, III)
- $c_2^A = \frac{\alpha_2 - \alpha_1}{2}$ (from III)
- c_3^A *free parameter*
- $c_4^A = A_{22}^{\mathrm{mrg}} - c_1^A \tanh(c_3^A)$ (from I)

- $c_1^\phi = \frac{(\omega_1 - \mathcal{M}_{\mathrm{BH}} \omega_{22}^{\mathrm{mrg}})(1 + c_3^\phi + c_4^\phi)}{c_2^\phi (c_3^\phi + 2c_4^\phi)}$ (from IV)
- $c_2^\phi = \alpha_2 - \alpha_1$ (from IV)
- c_3^ϕ *free parameter*
- c_4^ϕ *free parameter*